DILUTED MAGNETIC SEMICONDUCTOR EFFECTS IN Mn- AND Fe-IMPLANTED SILICON CARBIDE

A.V. KOMAROV,[1] A.V. LOS,[2] S.M. RYABCHENKO,[1] S.M. ROMANENKO[2]

[1]Institute of Physics, Nat. Acad. of Sci. of Ukraine
(46, Nauky Ave., Kyiv 03028, Ukraine)

[2]ISS Ltd., Semiconductors and Circuits Lab.,
(15, Bozhenko Str., Kyiv 03680, Ukraine)

PACS 78.20.Ls, 75.50.Pp, 61.80.Jh, 75.60.Ejx

Light transmission and Faraday rotation spectra measured at a temperature of 2 K for 4H–SiC and 6H–SiC single crystals of silicon carbide implanted with Mn and Fe ions, respectively, and for control specimens of the same single crystals not subjected to the implantation have been compared. A 190-keV beam is used to implant ions at the total exposure doses of 3.8×10^{16} and 5.5×10^{16} cm^{-2}. As a result, layers of about 0.2 μm in thickness doped with Mn or Fe ions to the average ionic concentration of about 10^{21} cm^{-3} emerged. Although the light transmission through implanted crystals is only slightly changed in comparison with that for the reference specimen, it corresponds to rather a high value of the light extinction coefficient in the implanted layer. Such a phenomenon is interpreted as a result of the light scattering by optical inhomogeneities created by high-energy ions in the surface layer. The presence of magnetic ions in the near-surface layer gives rise to noticeable changes in the Faraday rotation spectra of specimens. The estimated values of the Verdet constant for those layers turn out of the opposite sign and about three orders of magnitude larger than that for the undoped specimens. The dependences of the Faraday rotation contribution on the magnetic field for the Mn-implanted layer are found to get saturated, which evidences a proportionality between the Faraday rotation and the magnetization of the paramagnetic subsystem of Mn ions. In the case of a Fe-implanted layer, those dependences turn out linear, similar to what is observed for $A^{II}FeB^{IV}$ semimagnetic semiconductors. An assumption is made that Fe ions are in the singlet ground state in SiC and $A^{II}FeB^{IV}$ and become magnetized in an external field owing to a mechanism similar to the van Vleck one. The SiC layers with implanted Mn or Fe ions are found to reveal magnetooptical properties typical of diluted magnetic (semimagnetic) semiconductors. At the same time, no ferromagnetic ordering is observed in the studied (Si,Mn)C and (Si,Fe)C specimens.

1. Introduction

The search for new ferromagnetic (FM) semiconducting materials, the Curie temperature T_C of which would be higher than the room one, is an important problem for modern spintronics. An FM ordering in diluted magnetic (semimagnetic) semiconductors (DMS) induced by the interaction between charge carriers and doping magnetic ions was predicted in [1]. In [2], a possibility to achieve the T_C values higher than 300 K was forecasted for certain wide-gap DMSs with rather a high concentration of free holes. This prognosis gave impetus to plenty of experiments aimed at demonstrating DMS materials with high T_C. Many authors reported that they observed ferromagnetism in the corresponding objects at temperatures above room one. However, the most such observations turned out later to be a consequence of uncontrollable precipitates in the studied specimens or inclusions of other phases of transition metal (TM) compounds in solid solutions, to which DMS specimens belong [3]. In a number of materials, the ferromagnetic ordering was observed in the absence of charge carriers at a corresponding concentration in the specimens or even in the absence of transition metal ions. This circumstance stimulated the appearance of theoretical works, where the FM ordering in those specimens was explained as a result of other reasons different from the exchange interaction between charge carriers and doping magnetic ions. However, no progress was attained in this way to find materials that would combine the beneficial semiconducting properties and the FM ordering at temperatures necessary for the functioning of practical spintronic devices (see the analysis of this issue, e.g., in [3]). Nevertheless, the search for new materials (both semiconducting matrices and TM ions dissolved in them), which could be suitable for synthesizing DMSs with high temperatures of the FM ordering, remains challenging.

A relatively little attention has been paid till now to the studies of magnetic properties of SiC crystals with a wide forbidden gap doped with TM impurities. Early experimental researches testified to a FM response in Ni-, Mn-, and Fe-doped SiC, with T_C-values ranging in various specimens from rather low temperatures to those close to the ambient one [4–6]. The authors attributed the FM response to either the manifestation of a "genuine DMS" with FM ordering or the formation of secondary phases. Later, it was reported on a

ferromagnetic state of Cr-doped SiC with $T_C \approx 70$ K at a Cr concentration of 0.02 wt% [7] and about the FM ordering at a temperature above room one in amorphous SiC doped with Cr to a concentration of 7–10 at% [8]. In the researches of 6H–SiC implanted with Fe ions [5], a conclusion was drawn that the ferromagnetism of specimens observed in magnetostatic and Mössbauer effect measurements originates from superparamagnetic Fe_3Si inclusions or a small number of iron nanoparticle inclusions in the SiC matrix. The researches of Mn-implanted heteroepitaxial 3C–SiC/SiC structures [9] and carbon-incorporating SiMn films grown on 4H–SiC substrates [10], the structural, magnetic, and magnetooptical properties of Mn-doped SiC films prepared on 3C–SiC substrates [11], and the properties of 6H–SiC films low-doped with Mn [12] and polycrystalline 3C–SiC [13] testify that Mn can be a suitable impurity for achieving a high-temperature FM ordering in the SiC DMS. A similar conclusion was made in a number of theoretical researches of SiC doped with TM ions [14, 15]. In particular, the *ab initio* calculation [15] for SiC doped with Mn to a concentration of a few per cent predicted that the temperatures $T_C = 400$–500 K and above can be obtained for this class of materials.

The researches of DMSs, which have been carried out for many years, testify that magnetostatic studies (the measurements of magnetization curves) alone cannot allow one to unambiguously judge the nature of a studied magnetic material, which, unfortunately, is still often made while studying such materials. In our opinion, there are no reliable data for today that would prove the "genuine DMS nature" of FM manifestations observed in SiC specimens doped with TMs. Magnetooptical studies are one of the most reliable ways to establish whether the magnetic properties of an examined semiconductor doped with TM ions are governed by the solid solution (i.e., DMS) properties or they may originate from the presence of various phases or inclusions in synthesized specimens. The main features in the DMS behavior, including the FM ordering [1, 2], are known to be associated with the exchange interaction between free charge carriers and localized spins of TM ions inserted into a semiconductor. This interaction brings about a "giant" spin splitting of carrier band states and, accordingly, to a drastic growth in the magnetooptical response of DMSs. This phenomenon was widely studied for substances with a wide energy gap (see, e.g., works [16–19]). The magnetooptical effects associated with the giant spin splitting must demonstrate a characteristic spectral dependence related to the electron structure of the DMS under investigation. This dependence allows them to be distinguished from magnetooptical phenomena invoked by extraneous inclusions or crystal phases.

The aim of this research is to obtain new data on the magnetic, optical, and magnetooptical properties of SiC implanted with Mn and Fe ions and to check whether such materials demonstrate properties typical of DMS and, probably, the FM ordering. It should be noted that, unlike direct-band-gap DMSs, which were studied in works [16–19] and later ones, SiC (and, as it should be expected, the SiC-based DMSs) has an indirect-band-gap electronic structure. The researches of indirect-band-gap DMSs and their magnetooptical properties are poorly presented in the literature, being, therefore, of additional interest for the tasks of this work.

2. Specimens and Experimental Methods

The specimens to be studied in this work were prepared with the use of single-crystalline SiC substrates (from the Cree, Inc.). The substrate of a 4H–SiC crystal implanted with Mn ions had the thickness $d_0 = 415$ μm, conductivity of the p-type, and free carrier concentration of about 10^{18} cm^{-3}. The substrate of a p-conducting 6H–SiC crystal implanted with Fe ions had almost the same thickness $d = 417$ μm and the same free carrier concentration of about 10^{18} cm^{-3}. Doping with Mn and Fe ions was carried out by implanting them using ionic beams with an energy of 190 keV and at a temperature of 350 °C to avoid the amorphization. The total exposure doses were 3.8×10^{16} and 5.5×10^{16} cm^{-2}. The distribution profile of the implanted impurity calculated with the help of a profile code (Core Systems, Inc.) [21] for the case of the implantation with Mn ions to a dose of 3.8×10^{16} cm^{-2} is depicted in Fig. 1. The implantation gave rise to the formation of a layer, doped with corresponding ions, on the specimen surface. In the case exhibited in Fig. 1, the peak concentration of Mn ions in the layer reached 5×10^{21} cm^{-3}, which corresponded to the contents of those ions of approximately 5 at%. If the total exposure dose was 5.5×10^{16} cm^{-2}, the ion distribution profile over the depth was similar, with the peak concentration being 1.45 times higher. Similar profiles of the ion distribution were also obtained in the case of the implantation with Fe ions, with almost the same peak and average concentrations. The specimens implanted with corresponding TM ions, as well as the specimen not subjected to the implantation (it was cut off from the same substrate before the ion-beam irradiation and served as the reference one), were further annealed at

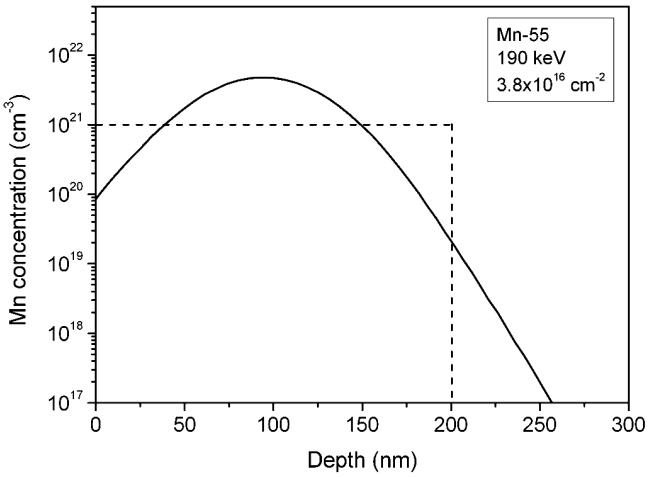

Fig. 1. Calculated concentration profile of Mn ions for a ionic beam energy of 190 keV and a total exposure dose of 3.8×10^{16} cm^{-2}. The vertical and horizontal dashed lines denote the boundaries of the effective layer of the depth $d_2 = 200$ nm with implanted Mn and an average Mn concentration of 10^{21} cm^{-3}, the concept of which is used further, while discussing the results obtained

1650 °C for 30 min. The back side of specimens was polished to make them transparent.

It is evident that the concentration of TM ions in the implanted layer is not uniform. However, for the simplicity of the subsequent analysis, we supposed that the implanted specimen consisted of two parts: a layer doped with ions (Mn or Fe), which was characterized by a constant effective concentration of the the impurity and a certain effective thickness (we denote it as d_1), and the main part, free of those ions, with all its properties being similar to those in the reference specimen, but a little thinner, $d_2 = d_0 - d_1$. We made a transmission electron microscopy (TEM) micrograph of the transverse cross-section of the near-surface layer in the specimen implanted with Mn ions (the photo was published in work [22], in which the first results of our researches dealing with (Si,Mn)C were reported). The micrograph allowed us to establish that the implantation of Mn ions into this layer was accompanied by the formation of particles 40–80 nm in dimension in the SiC matrix. The particles were observed at a depth down to 200–250 nm, and their maximum concentration was located by 80–90 nm below the specimen surface, where the Mn ion concentration was maximal. As such particles, there can be either Mn precipitates or nanogranules of secondary phases. A similar situation also arose at a doping with Fe ions by the implantation.

It was demonstrated in a number of researches [23, 24] that the Si sublattice in SiC is more favorable in comparison with the C one from the viewpoint of the substitution by paramagnetic ions. Therefore, we suppose that, after the ion implantation followed by the annealing, Mn and Fe atoms, which were not included into precipitates or secondary phases, substitute Si ions. Below, we denote the resulting solid solutions as (Si,Mn)C and (Si,Fe)C.

Concerning the manifestation of DMS properties, it seems reasonable that the thickness of the near-surface layer, in which the concentration of TM ions is not lower than 0.1 at%, and the exchange interaction between the localized magnetic moments of those ions by means of charge carriers is still effective, be selected as the effective thickness of a layer doped with TM ions. The value $d_1 = 200$ nm was determined on the basis of those speculations. It is marked in Fig. 1 and will be used further in calculations and the discussion.

The magnetization of specimens implanted with TM ions was measured at room temperature on a LDJ-9500 vibrating sample magnetometer. The measurements detected only an insignificant paramagnetic response. An estimation of the possible FM contribution, which could take place, provided that the layer implanted with those ions were ferromagnetic at 300 K, showed that it could be observed only at the device sensitivity threshold. It is a consequence of the fact that, although the concentration of TM ions in the implanted layer is rather high, the layer thickness and, as a consequence, the volume are very small. It is worth noting that we have no information concerning the charge state acquired by TM ions in SiC at the implantation. Therefore, we cannot say for sure which spins (magnetic moments) of ions are realized at that. However, irrespective of this uncertainty, we may assert that the ions concerned possess localized magnetic moments different from zero.

Three specimens were used in the measurements: the specimen with a (Si,Mn)C layer created by the ionic irradiation to a total exposure dose of 3.8×10^{16} cm^{-2} and two specimens with a (Si,Fe)C layer created by the ionic irradiation to total doses of 3.8×10^{16} and 5.5×10^{16} cm^{-2}, respectively.

For optical and magnetooptical measurements, a specimen was placed in a helium cryostat containing a superconducting solenoid with a magnetic field H up to 30 kOe directed along the light path. Measurements were carried out at the temperature $T = 2$ K. The cryostat was disposed between polarizers P_1 and P_2, the polarization planes of which could be regulated. Measurements for the specimen with the (Si,Mn)C layer were carried out on a StellarNet EPP2000C spectrophotometer, which operated in the photon energy range 1–7 eV with a resolution of 0.75 nm, which corresponded to an

energy resolution of 2.7–7.6 meV in the energy range 2–3.5 eV used by us. Measurements for the specimens with a (Si,Fe)C layer in the interval 2.98–3.22 eV were carried out on a DFS-12 grating spectrophotometer with a resolution of about 1 meV in the measurement interval.

SiC substrates are usually so cut out that the hexagonal axis C is slightly tilted with respect to the normal to the substrate surface. The specific value of the angle with respect to the axis depends, in particular, on the SiC polytype. In our case, it was equal to $7^\circ 56'$ for 4H-specimens and $3^\circ 31'$ for 6H-ones. It is of importance for the polarization measurements that light should propagate along the optical axis of a crystal. Therefore, the axis C of the specimen had to be oriented along the direction of a light beam. The measurements were carried out at the relative orientation $\mathbf{H} \parallel \mathbf{K} \parallel \mathbf{C}$ of the magnetic field $\mathbf{H}$, the light wave vector $\mathbf{K}$, and the specimen optical axis $\mathbf{C}$.

The optical density spectra $D(E)$ of the specimens were determined as usual,

$$D\,(E) = \log_{10}\left[I_0\,(E)\,/I_t\,(E)\right], \tag{1}$$

where $I_0\,(E)$ and $I_t\,(E)$ are the intensities of incident on and transmitted through the specimen, respectively, light with photon energy E. The dependence $D(E)$ was measured in the zero magnetic field. In the course of those measurements, polarizers P_1 and P_2 were either so arranged that their polarization planes coincided, or they were removed altogether. As a result, no difference was detected, to the measurement accuracy, between the $D(E)$-values obtained in polarized and non-polarized light. While measuring the dependence $I_0(E)$, the specimen was removed.

The spectral dependences of the Faraday rotation (FR) angle for the light polarization plane, $Q(E,H)$, were determined by measuring the intensity of light that passed through the specimen and through the polarizers crossed at the angle φ_0 between their polarization planes, when the magnetic field was switched on. In the measurements, we used the angle $\varphi_0 = 85^\circ$ for the specimen implanted with Mn ions and the angle $\varphi_0 = 45^\circ$ for the specimens implanted with Fe ions. The standard expression for $Q(E,H)$ in this case looks like

$$Q(E,H) = \arccos\sqrt{I(E,H)\,\cos^2(\varphi_0)/I(E,0)} - \varphi_0, \tag{2}$$

where $I(E,H)$ is the intensity of light transmitted through polarizers P_1 and P_2 and through the specimen; it depends on E- and H-values. The quantity $I(E,0)$ was measured without magnetic field, provided that the arrangement of the specimen, the polarizers, and other installation components was the same. Expression (2) is valid provided that (i) the specimen does not depolarize light that passes through it, (ii) $Q(E,H) < 90^\circ - \varphi_0$, and (iii) the specimen optical density is practically independent of the applied magnetic field. It was found that, for specimens, the optical c-axis of which was oriented exactly along the light propagation direction irrespective of whether $\varphi_0 = 85^\circ$ or 45°, the depolarization, both at $H = 0$ and $H \neq 0$, led to changes in the light intensity after passing the specimen and the polarizers, which were much smaller than the intensity change owing to the FR of light polarization plane in magnetic fields higher than a few kilooersteds. At the same time, the exact orientation of the optical axis of a specimen along the light incidence direction was important for avoiding errors at measurements. Within the range of applied magnetic fields, the optical density of specimens did not depend on H within the accuracy of measurements, whereas the absolute values of $Q(E,H)$ turned out smaller than $90^\circ - \varphi_0$ at both used φ_0-values. Hence, the aforementioned conditions for the applicability of Eq. (2) were satisfied. Making allowance for probable errors at orienting the specimen optical axis, the depolarization of light at its passage through the optical elements of the installation, and the magnitude of signal-to-noise ratio obtained at the measurements, we estimated the determination error limits δQ for the FR angle measured on a StellarNet EPP2000C installation as $\delta Q = \pm 0.1^\circ$ at $D(E) < 1$. For a lower relative intensity of the light transmitted through the specimen, the error is larger. According to our estimations, $\delta Q = \pm 0.5^\circ$ at $D(E) \approx 3$. For measurements on a DFS-12 spectrophotometer, this error reached the value $\delta Q = \pm 0.5^\circ$ at $D(E) < 1$.

The differences in the optical and magnetooptical properties of implanted specimens and the reference one were interpreted by us as a consequence of modifications in the near-surface layer of 6H– or 4H–SiC stimulated by the implantation of TM ions into it, which enabled us to determine the optical density of this layer and the FR angle in it in terms of the difference between the characteristics of implanted and reference specimens.

To discuss the influence of doping SiC with TM ions on its optical and magnetooptical properties, we use standard characteristics of the crystal, such as the "decimal absorption coefficient" $k_d(E)$ and the Verdet constant of the material $V(E)$:

$$k_d(E) = D(E)/d, \tag{3}$$

$$V(E) = Q(E,H)/(H\,d), \tag{4}$$

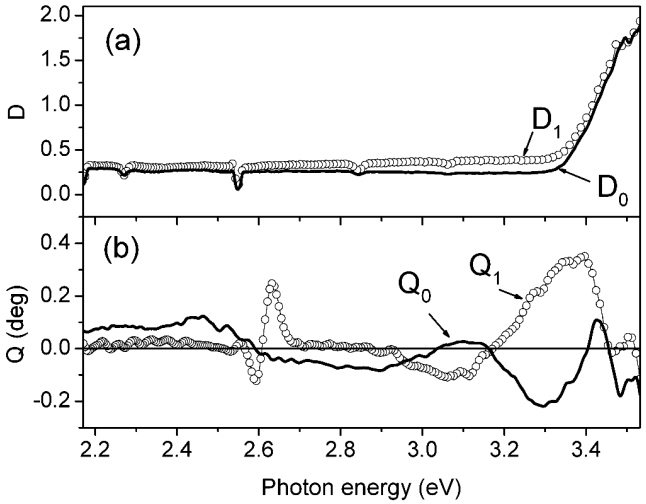

Fig. 2. Spectral dependences of (a) the optical density and (b) the angle of Faraday rotation in 4H–SiC specimens: reference one (D_0 and Q_0) and the specimen implanted with Mn ions (D_1 and Q_1). Measurements were carried out at $T = 2$ K in the magnetic fields $H = 0$ for $D_0(E)$ and $D_1(E)$ and $H = 25$ kOe for $Q_0(E)$ and $Q_1(E)$

where d is the optical path length passed by light in the crystal (the crystal thickness). Both $k_d(E)$ and $V(E)$ depend on the temperature. The decimal absorption coefficient and the Verdet constant of the reference specimen will be denoted as k_0 and V_0, respectively. In the adopted model, we consider a specimen implanted with TM ions as if it consisted of two uniform layers – implanted and non-implanted ones – d_1 and d_2 in thickness, respectively. The latter layer will be described using the same parameters as for the reference specimen, i.e. k_0 and V_0. The decimal absorption coefficient and the Verdet constant of the layer implanted with TM ions are denoted as k_1 and V_1, respectively. Then, the functions $D_1(E)$ and $Q_1(E, H)$ are the sums of contributions made by those two layers, and they can be described as follows:

$$D_1(E) = d_1 k_1(E) + d_2 k_0(E), \tag{5}$$

$$Q_1(E, H) = H[d_1 V_1(E) + d_2 V_0(E)]. \tag{6}$$

Combining Eqs. (5) and (6) with expressions (3) and (4) written down for the reference specimen, we can extract $k_1(E)$ and $V_1(E)$ from the data for $D_0(E)$, $D_1(E)$ and $Q_0(E)$, $Q_1(E)$, respectively:

$$k_1(E) = \frac{1}{d_1}\left[D_1(E) - D_0(E)\frac{d_2}{d_1 + d_2}\right], \tag{7}$$

$$V_1(E) = \frac{1}{d_1 H}\left[Q_1(E) - Q_0(E)\frac{d_2}{d_1 + d_2}\right]. \tag{8}$$

3. Results of Optical and Magnetooptical Measurements

3.1. SiC crystals implanted with Mn ions

The spectral dependences of optical density for the reference 4H–SiC specimen and the 4H–SiC specimen implanted with Mn ions ($D_0(E)$ and $D_1(E)$, respectively) are shown in Fig. 2,a. One can see that the optical density differs very insignificantly for those two specimens in the whole interval of the applied light photon energy. The start of the absorption edge in the reference specimen at energies of 3.29–3.3 eV agrees with the measurement data for the width of the indirect energy gap in 4H–SiC at helium temperatures [25, 26]. Note that, in the energy range above 3.3 eV, there emerges the absorption in 4H–SiC by means of indirect optical transitions between the valence band maximum at point Γ and the lowest minimum in the conduction band group at point M in the Brillouin zone [27]. At lower energies, the spectrum is formed by direct transitions between impurity and defect states in the energy gap, including shallow donors and acceptors, on the one hand, and states in the allowed bands, on the other hand [28, 29].

There are the rather narrow peculiarities in the $D_1(E)$- and $D_0(E)$-curves at energies of 3.06, 2.84, 2.55, and 2.27 eV. We determined that they are associated with the properties of the installation used and, therefore, should be excluded from consideration.

Figure 2,b depicts the FR spectra $Q_1(E)$ and $Q_0(E)$ for the implanted and reference, respectively, specimens, which were measured in the magnetic field $H = 25$ kOe. It is evident that they are comparable with respect to the absolute values of rotation angle for the light polarization plane, although being considerably different by their spectral dependence forms and the rotation signs in various intervals of the analyzed spectral range. In particular, there appears a dispersion-like peculiarity of $Q_1(E)$ in rather a narrow energy interval from 2.5 to 2.7 eV centered at 2.61 ± 0.01 eV. This peculiarity is similar to that, which could arise as a consequence of the optical transition at this energy with a line half-width of approximately 0.1 eV; however, the origin of this transition is not clear now. The peculiarity concerned is available in the spectrum of the specimen implanted with Mn ions, but it is absent from the spectrum of the reference one. Therefore, it may probably be related to transitions associated with Mn ions (e.g., one

of $3d$–$3d$ transitions), Mn-containing defects, or defects induced by the implantation. We do not know reports on the optical transitions in Mn-doped SiC at such a photon energy.

While examining the dependences $Q_1(E)$ and $Q_0(E)$, it is evident that they are nonmonotonous. At the same time, on the scale of Fig. 2,*a*, there are no appreciable peculiarities in the $D_1(E)$ and $D_0(E)$ spectra, neither near an energy of 2.61 eV (it is the mentioned peculiarity in $Q_1(E)$), nor in other photon energy regions, where the spectrum of FR of the light polarization plane either is nonmonotonous or crosses zero. To summarize, note that the implantation of Mn ions led to an appreciable change in the magnetooptical activity of 4H–SiC, whereas the variation of optical properties, although taking place, is much less. These variations in optical and magnetooptical properties should be regarded as a result of modifications in the near-surface layer of 4H–SiC induced by the Mn-ion implantation, despite that the layer thickness, $d_1 = 0.2$ μm, is very small in comparison with the specimen one, $d_0 = 415$ μm.

In Fig. 3, the spectra of the decimal absorption coefficients for the reference specimen, $k_0(E)$, and the near-surface layer implanted with Mn ions, $k_1(E)$, are exhibited. They were calculated with the use of the dependences $D_0(E)$ and $D_1(E)$ (Fig. 2,*a*), as well as Eqs. (3) and (7). The curve $k_0(E)$ in Fig. 3,*a*, as well as the curve $D_0(E)$ in Fig. 2,*a*, does not reveal any peculiarities in the energy range from 2.2 to 3.3 eV, but narrow cusps. The latter were induced by the measurement installation, and, as was already indicated, they should be excluded from consideration. Narrow decreases in $k_1(E)$ (Fig. 3,*b*) at energies of about 2.27, 2.55, 2.84, and 3.06 eV are also associated with the experimental installation, and they should not be paid attention to.

In contrast to the curve $k_0(E)$, the curve $k_1(E)$ includes a wide asymmetric feature with a maximum at 3.2 ± 0.1 eV, and rather a high coefficient of light extinction corresponds to it. The expected relative error of calculations for $k_1(E)$ amounts to $\delta k_1/k_1 \approx \delta D/|D_1 - D_0|$, where δD is the measurement error for the optical density. The value of $\delta k_1/k_1$ can be large enough in the absorption edge region, where D_1 and D_0 are close to each other (see Fig. 2). At the same time, the calculated value of the $k_1(E)$-maximum in the range of 3.2 ± 0.1 eV is much higher than the estimated probable error. An abnormal intensity in the maximum and its large width raise doubts that the extinction of light in the layer described by the function $k_1(E)$ originates from optical transitions that appear in this energy range as a result of the Mn-ion implantation. It seems more probable that

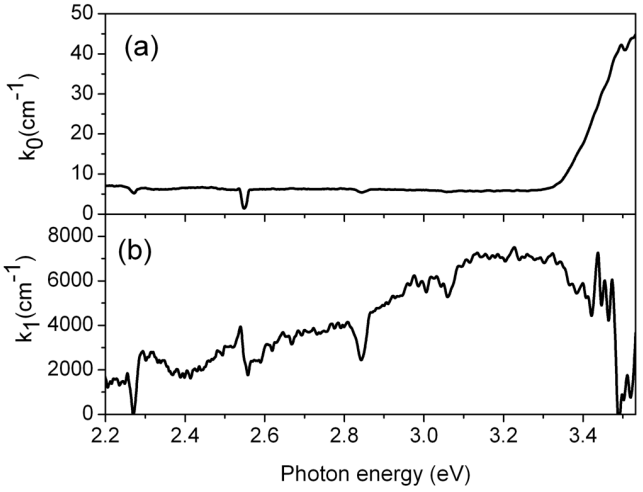

Fig. 3. Spectral dependences of the decimal light-absorption coefficient for (*a*) the reference specimen and (*b*) the layer implanted with Mn ions calculated using the data of Fig. 2,*a* and Eqs. (3) and (7)

this extinction is associated with the light scattering by inhomogeneities created in the near-surface layer irradiated with Mn ions and not completely removed at the annealing, or Mn clusters, or secondary phase inclusions. The estimation shows that the intense scattering in this energy range can be induced by inhomogeneities 50–90 nm in dimension, whose presence as a consequence of the intense implantation and the formation of clusters is quite probable, as was discussed earlier. As was already mentioned, no appreciable depolarization was observed for light transmitted through the specimen implanted with Mn ions. This circumstance does not necessarily contradict the idea of light scattering in the implanted layer, because the magnitude of light extinction in such a thin layer is small, despite the large values of extinction factor k_1, which we associate with the scattering process. However, an unequivocal elucidation of why the observed coefficient of light extinction in a Mn-doped layer is large demands additional researches.

In Fig. 4, the spectra of the Verdet constant for the reference specimen, V_0, and the layer implanted with Mn ions, V_1, are depicted. They were calculated from the spectra $Q_0(E,H)$ and $Q_1(E,H)$ (Fig. 2,*b*) with the use of Eqs. (4) and (8). The shape of the spectral dependence $V_0(E)$ in the interval adjacent to the start of the absorption edge depends on the structure of the magnetic-field-induced splitting of absorption bands in this region into the circularly polarized $\sigma^{(+)}$- and $\sigma^{(-)}$-components, as well as on the contribution to the transparency region made by indirect band-to-band transitions. All features

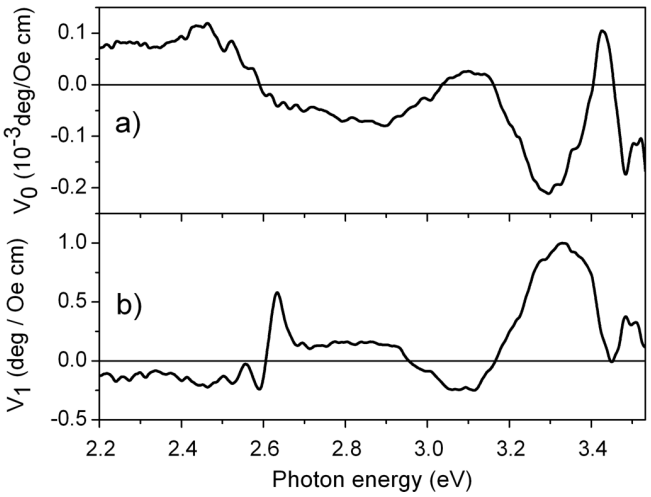

Fig. 4. Spectra of the Verdet constant for (*a*) the reference specimen and (*b*) the layer implanted with Mn ions calculated using the data of Fig. 2 and Eqs. (4) and (8)

in the spectral dependence of the Verdet constant on the aforementioned factors are governed by the parameters of Zeeman interaction of photoexcited charge carriers in both the lowest conduction band and the upper valence band of the reference 4H–SiC crystal with the external magnetic field H, as well as by the parameters of Zeeman splitting of the impurity absorption bands, in the corresponding spectral range. Not going deeper into the interpretation of the features in the spectral dependence of the Verdet constant, let us pay attention to the shape of the plot $V_0(E)$ presented in Fig. 4,*a*. In the energy interval from 2.2 to 3.3 eV, this curve is nonmonotonous and can be roughly presented in the form of a sum of three very wide dispersion contours, the FR changing its sign in each of them. It could be interpreted as a manifestation of the Verdet constant dispersion in the region that includes three wide absorption bands with the maxima fixed at energies corresponding to the points, where $V_0(E)$ changes its sign. Unfortunately, we do not have enough data to connect this model with the spectrum of absorption by defects and impurities in 4H–SiC in the interval that precedes the absorption edge. However, we may consider that the found structure of the spectral dependence $V_0(E)$ is connected just with direct transitions of this kind.

Concerning the contribution to $V_0(E)$ from indirect band-to-band transitions in the transparency interval, Figs. 2 and 3 demonstrate that no appreciable dispersion of the Verdet constant is observed, which would be reciprocal to the spectral detuning between the start of the indirect edge absorption and the energy of light quanta E. Such a contribution would have been present, if the absorption edge had been formed by direct transitions. At the same time, in accordance with works [30–32], the spectral dependence of the contribution made by interband transitions to the Faraday effect in the transparency range of indirect-band-gap semiconductors includes two components. One of them is connected with indirect phonon-induced band-to-band transitions and the other with hypothetical direct transitions from the valence band maximum into a state in the conduction band with the same wave vector. The spectral dependence of the former contribution tends to a constant value at the indirect absorption edge. For the latter, it is reciprocal to a certain power of the energy difference between the incident photon and the hypothetical direct transition. Therefore, for 4H–SiC, where the energy of the mentioned "direct transition" amounts to 5–6 eV [27], which is well above the indirect transition edge, one should not expect a strong spectral dependence of each of those contributions to the FR in the spectral interval studied here.

The most remarkable feature in the spectral dependence $V_1(E)$ shown in Fig. 4,*b* is a relatively narrow dispersion contour in a vicinity of 2.6 eV. The remaining part of the dependence reminds $V_0(E)$ by its profile, but the signs of V_1 and V_0 are different. However, the main difference between those dependences consists in that the absolute values of V_1 exceed those of V_0 by more than two orders of magnitude. Such a strong enhancement of the magnetooptical activity in the near-surface layer of a SiC crystal implanted with Mn ions can be explained by the fact that not only the applied magnetic field affects the photoexcited carriers (free or which are components of various centers) in it, but also the exchange fields of interaction between the carriers and the localized spins of Mn ions implanted into the layer. The corresponding giant enhancement of magnetooptical effects is well-known in the physics of DMSs (see, e.g., works [16–20, 33]). In DMSs, the effective exchange field is proportional to the magnetization of the subsystem of localized magnetic moments in the applied magnetic field at a given temperature. The exchange fields acting on electrons in the conduction and valence bands turn out much stronger than the external magnetic field. Electrons belonging to different centers and taking part in transitions near the absorption edge can undergo, of course, the action of different exchange fields, depending on the radius of a state of carriers in those centers. In Fig. 4 exhibiting the plots for Verdet constants, the bands corresponding to different probable centers are not resolved. Therefore, it is hardly expedient to discuss the details of probable

models of centers, which are known to exist in 4H–SiC, as well as the possible differences in the enhancements of magnetooptical effects at optical transitions in them when introducing magnetic ions into the crystal, at the present stage.

In order to estimate the enhancement of magnetooptical effects in the layer with Mn ions with respect to the case of ion-free crystal, we can consider and compare the sections of the plots $V_1(E)$ and $V_0(E)$ in the energy interval from 2.9 to 3.4 eV. Here, the curves resemble the wide dispersion contours typical of spectral dependences for the Verdet constant in a vicinity of optical transitions. Suppose that such peculiarities preserve their behavior for similar transitions in both the Mn-doped layer and the reference specimen. Then, the ratio between the amplitudes of those dispersion curves, $|\Delta V_1| / |\Delta V_0|$, can evaluate the growth of the absolute value of effective magnetic field in comparison with the external one. Such an evaluation for the peculiarity in the interval 2.9–3.4 eV brings about $|\Delta V_1| / |\Delta V_0| \approx 5 \times 10^3$. The same evaluation for the peculiarity in a vicinity of 2.4–2.8 eV (except the narrow dispersion contour V_1 in between 2.55 and 2.67 eV) gives $|\Delta V_1| / |\Delta V_0| \approx 1.02 \times 10^3$. These ratios are identical by magnitude to those observed for DMSs of the $A^{II}MnB^{VI}$ type (see works [2, 16–20] and others devoted to those DMSs). An "approximate sign inversion" between $V_1(E)$ and $V_0(E)$ testifies that the antiferromagnetic exchange interaction of one of the carriers (in the ground or excited state) with Mn ions dominates in the "giant enhancement" of the Faraday magnetooptical effect in the 4H–SiC layer with implanted Mn ions. It should also be noticed that both spectra, $V_1(E)$ and $V_0(E)$, do not reveal an appreciable component, which would be reciprocal to the quantum energy detuning with respect to the absorption edge, which is a consequence of the indirect-band-gap nature of this absorption in both the reference 4H–SiC specimen and the DMS on its basis created under the implantation of Mn ions.

The effective internal magnetic field in DMSs that acts on free charge carriers is proportional to the magnetization of the subsystem of localized magnetic-ion moments. If the subsystem is in the paramagnetic state, the dependence of its magnetization on the external field should get saturated in large enough magnetic fields even at low temperatures. Then, the FR will also get saturated or, after the saturation, even decrease as the external field grows further, if the effective (exchange) and applied magnetic fields are of opposite signs. In other words, the "Verdet constant" will depend on the external field. At the same time, the FR in a crystal without magnetic ions has to follow the linear dependence on the applied field. In this case, the "Verdet constant" is a genuine constant. If the DMS layer is FM-ordered, its contribution to the FR has to manifest itself even without external magnetic field: either as a FR different from zero or as an appreciable depolarization of transmitted light, depending on whether the layer is single- or multidomain. Both those effects depend on the orientation of the spontaneous magnetization in the FM ordered layer or on its domain structure. The both should get saturated in low magnetic fields, which saturate the magnetization of this layer in the FM state. Those speculations can be used to test, if a "giant" enhancement of $V_1(E)$, in comparison with that of $V_0(E)$, takes place owing to the exchange interaction between charge carriers and magnetic ions in the DMS created by the Mn-ion implantation, as well as to test which is the state of this layer, paramagnetic or ferromagnetic.

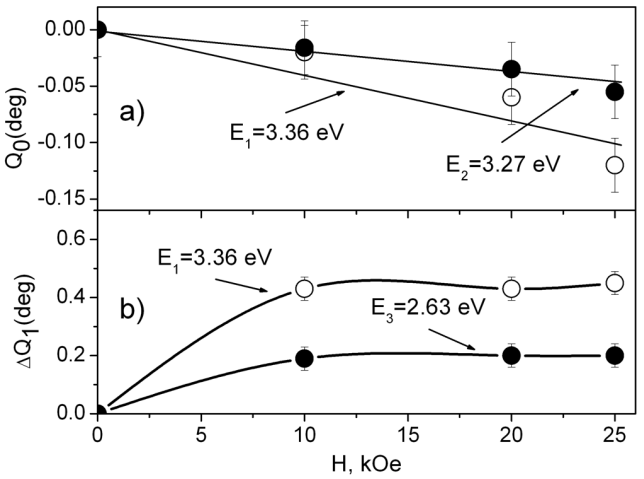

Fig. 5. Dependences of the FR angle on the magnetic field for two energies of incident-light quanta: (*a*) for the reference 4H–SiC specimen and (*b*) for the near-surface layer with Mn ions Mn (calculated with the use of Eq. (9))

In Fig. 5, the dependences of the FR angle in the reference specimen, $Q_0\,(E, H)$, and the contribution to the rotation angle from the layer containing Mn ions in the implanted specimen, $\Delta Q_1\,(E, H)$, on the magnetic field are depicted for two photon energies E. The quantity $\Delta Q_1(E,H)$ was calculated using the values for $Q_1(E,H)$ and $Q_0(E,H)$, and the relation

$$\Delta Q_1\,(E,\, H) = Q_1\,(E, H) - Q_0\,(E, H)\, d_2/d_0. \qquad (9)$$

The Q_0- and ΔQ_1-values shown in Fig. 5 are comparable with each other by magnitude, although V_1 is much larger than V_0 (see Fig. 4). It is a consequence of a small thickness of the layer that contains Mn ions. The

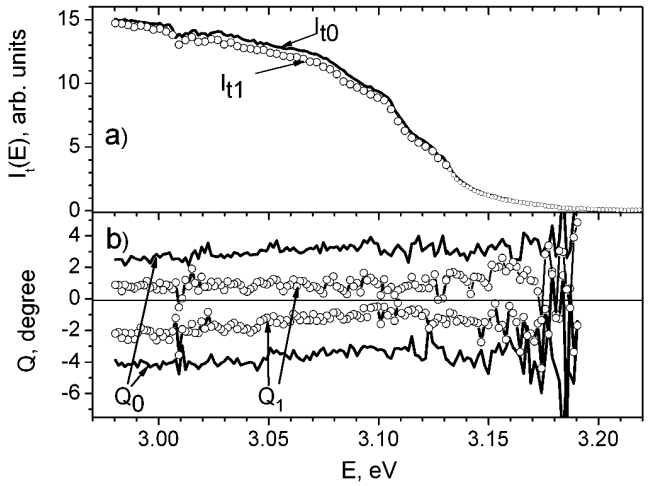

Fig. 6. (*a*) Curves of light transmittances through the reference specimen (solid curve, I_{t0}) and the specimen implanted with Fe ions to a dose of 5.5×10^{16} cm^{-2} (hollow circles, I_{t1}); (*b*) rotation angles of the light-polarization plane in the 20-kOe fields ("+" and "−") for the reference specimen (Q_0, solid curves) and the specimen implanted with Fe ions (Q_1, hollow circles). Curves with the rotation angles $Q > 0$ and $Q < 0$ for each specimen correspond to the opposite directions of the applied field

relative error in the determination of ΔQ_1 is equal to $\delta\Delta Q_1/\Delta Q_1 \approx \delta\,|Q_1 - Q_0|\,/\,|Q_1 - Q_0| \approx 2\delta Q_{0,1}/Q_{0,1}$, i.e. it is almost the same as the error in the determination of the FR angle.

Figure 5,*a* demonstrates that the dependence $Q_0(E, H)$ is linear in the magnetic field, and the Verdet constant V_0 does not depend on H. At the same time, the magnetic-field dependences $\Delta Q_1(E,\ H)$ get saturated in high enough fields at both photon energies. Therefore, the FR in the layer with Mn ions is proportional to the magnetization of the paramagnetic system. This fact should be considered as an essential argument in favor of our hypothesis concerning the reasons for the "giant" increase of the Faraday rotation in a layer with introduced Mn ions. It should be noted that one of the curves in Fig. 5,*b* corresponds to a photon energy of 2.63 eV, which corresponds to the maximum of the relatively narrow dispersion-type peculiarity in $V_1(E)$ (in the energy interval from 2.55 to 2.68 eV), which has no analog in the corresponding dependence for the reference specimen. This curve gets also saturated, which additionally confirms our assumption that this peculiarity is associated with centers created in the layer by Mn ions.

Our measurements also showed that, without applied magnetic field, no rotation of the polarization plane of transmitted light and no considerable light depolarization were observed in the whole spectral range of measurements, whereas the saturation field for FR was rather high. Therefore, we may draw conclusions that the layer created at the implantation of Mn ions makes a considerable contribution to the observed FR, this layer has the properties of a DMS, but it is not ferromagnetic even at $T = 2$ K.

3.2. SiC crystals implanted with Fe ions

6H–SiC crystals implanted with Fe ions were studied in a somewhat narrower spectral interval. The major qualitative results turned out similar to those obtained for the 4H–SiC specimen implanted with Mn ions. Therefore, we report them, by only indicating the detected differences between those two cases and without describing the analysis of results in such details, as it was done for the previous specimen. Figure 6,*a* demonstrates the curves of light transmission through the 6H–SiC specimen implanted with Fe ions and the reference 6H–SiC specimen. The latter is no more than a part of the same substrate, but not subjected to implantation. Figure 6,*b* presents the measurement results for the FR angle in the polarization plane of light that passes through the specimen. The angles were measured at two opposite directions of the field with respect to the light propagation direction.

The light transmission spectra for the reference and Fe-implanted specimens diminish in a vicinity of the indirect transition edge, with the light transmittance through the implanted specimen being slightly less than that through the reference one: approximately by as much as it was in the case of the specimen implanted with Mn ions. Note that the transmittance reduction with the growth of the photon energy occurs some earlier than it was in the case of 4H–SiC specimens. This circumstance corresponds to the fact that the indirect forbidden gap in 6H–SiC is narrower than that in 4H–SiC. According to various literature data, it amounts to 3.02–3.10 eV at helium temperatures (see, e.g., work [34]). The curves I_{t0} and I_{t1} in Fig. 6,*a* drastically fall down at $E = 3.12$ eV, that agrees in essence with those data.

The FR curves for the reference and implanted specimens demonstrate the same tendency as it was in the case of the specimen implanted with Mn ions. The layer implanted with Fe ions gives a contribution to the total rotation angle that is comparable by magnitude with that for the reference specimen, but is inverse by the sign. Taking into account that the thickness of this layer is approximately 800 times narrower than that of the ref-

erence specimen ($d_1/d_0 \approx 800$), we arrive at a conclusion that the FR was approximately identically enhanced in this layer as it was in the case of (Si,Mn)C layer, and that the sign of the effective field responsible for this enhancement is inverse to that of the external field. Attention is drawn by the fact that the absolute values of FR angles turned out considerably larger for 6H–SiC specimens, both the reference and Fe-doped ones, than for 4H–SiC specimens used for Mn-ion implantation. The origin of this difference still remains unclear and needs more detailed researches.

The FR dependences on the magnetic field for specimens implanted with Fe ions turned out qualitatively different from their counterparts for specimens implanted with Mn ions. In Fig. 7, they are depicted for the 6H–SiC specimen implanted with Fe ions to a total exposure dose of 3.8×10^{16} cm^{-2}. The curves were measured at $T = 2$ K and a light quantum energy of 3.122 eV. One can see that the difference between the polarization-plane rotation angles for the reference, $Q_0(H)$, and implanted, $Q_1(H)$, specimens does not saturate, which is in contrast to what was observed in the case of the implantation with Mn ions. Does it contradict the idea of the effective field describing the charge carrier–ion exchange interaction, which is proportional to the magnetization of the subsystem of paramagnetic ions in a DMS? From the researches of DMSs belonging to the $A^{II}FeB^{VI}$ group (see, e.g., work [35]), it is known that Fe^{2+} ions in the tetrahedral field of the crystal are in the singlet ground state [36], and their magnetization is governed by the van Vleck contribution owing to the hybridization with states with higher energy. As a consequence, the magnetization of the paramagnetic spin system Fe^{2+} in the tetrahedral field of $A^{II}FeB^{VI}$ compounds is linear in the field at low temperatures, being almost temperature-independent. We do possess definite data on the charge state of Fe ions in 6H–SiC. However, if a significant fraction of those ions were in the Fe^{2+} state, the situation in (Si,Fe)C DMSs would be similar to that in $A^{II}FeB^{VI}$. Hence, in our opinion, this difference between the FR dependences on the magnetic field in 6H–(Si,Fe)C and 4H–(Si,Mn)C follows from the difference between the ground energy states of Fe and Mn ions in SiC rather from the difference between the polytypes.

At the same time, the observable linear dependence of the FR difference between the reference specimen and the specimen containing a 6H–SiC layer doped with Fe ions on the magnetic field testifies to the absence of FM ordering in this layer at a temperature of 2 K.

Hence, although the researches of 6H–SiC specimens implanted with Fe ions left some issues to be studied further, the main conclusions can be drawn. First, the (Si,Fe)C layer formed under the implantation reveals typical DMS properties. It is also true for the (Si,Mn)C layer. Second, the layer remains paramagnetic even at $T = 2$ K at used Fe concentrations in it.

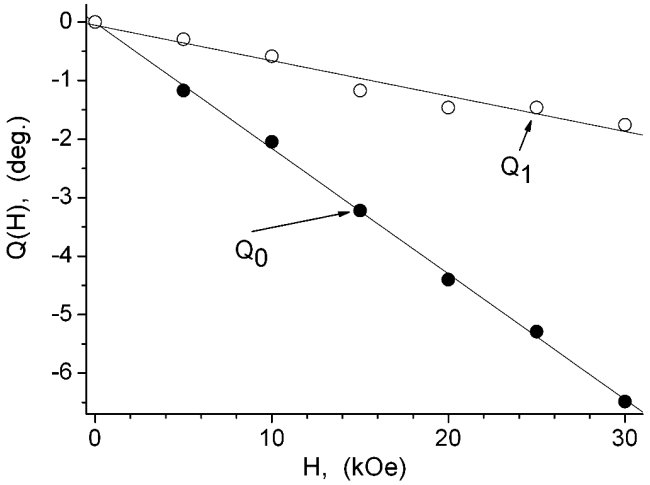

Fig. 7. Dependences of the FR angle of the magnetic field for the reference specimen, $Q_0(E, H)$, and the specimen implanted with Fe ions to a total exposure dose of 3.8×10^{16} cm^{-2}, $Q_1(E, H)$, measured at $T = 2$ K and $E = 3.122$ eV

4. Conclusions

The magnetic, optical, and magnetooptical properties of 4H–SiC and 6H–SiC single crystals implanted with Mn and Fe, respectively, ions within a thin ($d_1 \approx 0.20$ μm) layer at their surfaces have been studied. The peak concentration of relevant magnetic ions in this layer was approximately 5 at% or 5×10^{21} cm^{-3}, whereas the average effective concentration was evaluated as 1 at% or 10^{21} cm^{-3}. Electron microscopy data for implanted layers showed that some part of introduced ions may form clusters or inclusions of secondary phases in the near-surface region, where the concentration of introduced ions was maximal. It was found that, for both the 4H–SiC layer with implanted Mn ions and the 6H–SiC layer with Fe ions, the Faraday rotation of the light polarization plane normalized by a layer thickness drastically grows in comparison with the reference data for the non-implanted crystal. A "giant" enhancement of magnetooptical effects, similar to the observed one, is known from the physics of diluted magnetic (semimagnetic) semiconductors. The estimation of the Faraday effect enhancement in the studied SiC layers and a comparison with the same effect in reference specimens, which did not contain magnetic ions, gave rise to the ratio of

about 10^3 between the corresponding Verdet constants, which is comparable with the Faraday effect enhancement reported for DMSs belonging to the $A^{II}MnB^{VI}$ group. It gives ground to consider that the implantation of transition-metal ions forms the state of a diluted magnetic semiconductor in the corresponding SiC. The dependence of the Faraday rotation angle in the layer containing Mn ions on the magnetic field is found to get saturated at $T = 2$ K in relatively high fields, which testifies to the proportionality between the Faraday rotation in this layer and the magnetization of the paramagnetic subsystem of localized magnetic moments of Mn ions. At the same time, the difference between the Faraday rotation angles for the reference specimen and the specimen containing the (Si,Fe)C layer in the same field is linear in the field, similarly to what takes place in $A^{II}_{1-x}Fe_xB^{IV}$ compounds, where Fe^{2+} ions are in the singlet ground state in the tetrahedral field of the crystalline environment and, in a magnetic field, acquire the van Vleck magnetization, which is linear in the field, but temperature-independent in a certain interval of low temperatures. An assumption was made that the majority of ferrum ions in the formed, in our case, (Si,Fe)C layer are also in the Fe^{2+} state.

The spectral dependence of the Faraday rotation angle in the 4H–SiC and 6H–SiC layers implanted with Mn and Fe, respectively, ions does not contain a component that would be reciprocal to the detuning of the photon energy at the measurement point with respect to the absorption edge; the phenomenon has to be observed in the case of direct-band-gap DMSs. This fact testifies that DMSs created in SiC by the implantation of Mn and Fe ions remain indirect-band-gap semiconductors, as the initial SiC was.

Although the microscopic structure of the layers implanted with ions has not been analyzed in detail, we may draw a conclusion that the ferromagnetic ordering is not realized in both (Si,Mn)C and (Si,Fe) DMSs, at least at an effective concentration of corresponding ions of 10^{21} cm^{-3}, the latter being presumably reduced by the formation of precipitates and/or secondary phases. Notice that, to our knowledge, the presented research is a pioneering one dealing with the effects of exchange interaction between free charge carriers and a subsystem of localized magnetic moments in SiC DMSs. Further researches are needed to elucidate the nature of the magnetism in this complicated class of materials.

Our research was partially supported by the National Academy of Sciences of Ukraine in the framework of the projects BC-138/19 and BC-157/19.

1. E.A. Pashitskii and S.M. Ryabchenko, Sov. Phys. Solid State **21**, 322 (1979).
2. T. Dietl, H. Ohno, and F. Matsukura, Phys. Rev. B **63**, 195205 (2001).
3. A. Bonanni and T. Dietl, Chem. Soc. Rev. **39**, 528 (2010).
4. N. Theodoropoulou, A.F. Hebard, S.N.G. Chu, M.E. Overberg, C.R. Abernathy, S.J. Pearton, R.G. Wilson, J.M. Zavada, and Y.D. Park, J. Vac. Sci. Technol. A **20**, 579 (2002).
5. M. Syväjärvi, V. Stanciu, M. Izadifard, W.M. Chen, I.A. Buyanova, P. Svedlindh, and R. Yakimova, Mater. Sci. Forum **457-460**, 747 (2004).
6. F. Stromberg, W. Keune, X. Chen, S. Bedanta, H. Reuther, and A. Mücklich, J. Phys.: Condens. Matter **18**, 9881 (2006).
7. Zhao Huang and Qianwang Chen, J. Magn. Magn. Mater. **313**, 111 (2007).
8. C.G. Jin, X.M. Wu, L.J. Zhuge, Z.D. Sha, and B. Hong, J. Phys. D **41**, 035005 (2008).
9. K. Bouziane, M. Mamor, M. Elzain, Ph. Djemia, and S.M. Chérif, Phys. Rev. B **78**, 195305 (2008).
10. W. Wang, F. Takano, H. Akinaga, and H. Ofuchi, Phys. Rev. B **75**, 165323 (2007).
11. W. Wang, F. Takano, H. Ofuchi, and H. Akinaga, New J. Phys. **10**, 055006 (2008).
12. B. Song, H. Bao, H. Li, M. Lei, J. Jian, J. Han, X. Zhang, S. Meng, W. Wang, and X. Chen, Appl. Phys. Lett. **94**, 102508 (2009).
13. S. Ma, Y. Sun, B. Zhao, P. Tong, X. Zhu, and W. Song, Physica B **394**, (2007).
14. M.S. Miao and W.R.L. Lambrecht, Phys. Rev. B **74**, 235218 (2006).
15. A. Los and V. Los, J. Phys: Condens. Matter, **22**, 245801 (2010).
16. A.V. Komarov, S.M. Ryabchenko, I.I. Zheru, R.D. Ivanchuk, and O.V. Terletskij, Sov. Phys. JETP **46**, 318 (1977).
17. A.V. Komarov, S.M. Ryabchenko, and N.I. Vitrikhovskii, JETP Lett. **27**, 413 (1978).
18. J.A. Gaj, R.R. Galazka, and M. Nawrocki, Solid State Commun. **25**, 193 (1978).
19. J.A. Gaj, P. Buszewski, M.Z. Cieplak, G. Fishman, R.R. Galazka, J. Ginter, and M. Nawrocki, in *Proceedings of the 14-th International Conference on Physics of Semiconductors, Edinburg, 1978,* edited by B.L.H. Wilson (Institute of Physics, Bristol, 1978), p. 1113.

20. *Diluted Magnetic Semiconductors, Vol. 25: Semiconductors and Semimetals,* edited by J.K. Furdyna and J. Kossut (Academic Press, New York, 1988).

21. Core Systems, Inc., 1050, Kifer Road, Sunnyvale, CA 94086, USA.

22. A.V. Komarov, A.V. Los, S.M. Ryabchenko, and S.M. Romanenko, J. Appl. Phys. **109**, 083936 (2011).

23. V.A. Gubanov, C. Boekema, and C.Y. Fong, Appl. Phys. Lett. **78**, 216 (2001).

24. M.S. Miao, W.R.L. Lambrecht, Phys. Rev. B **68**, 125204 (2003).

25. W.J. Choyke, Mater. Res. Bull. **4**, 141 (1969).

26. L. Patrick, W.J. Choyke, and D.R. Hamilton, Phys. Rev. **137A**, 1515 (1965).

27. C. Persson and U. Lindefelt, J. Appl. Phys. **82**, 5496 (1997).

28. J.A. Freitas, jr., in *Properties of Silicon Carbide,* edited by G.L. Harris, EMIS Datareviews Series N 13, 29 (1995).

29. G. Pensl and W.J. Choyke, Physica B **185**, 264 (1993).

30. I.M. Boswarva, R.E. Howard and A.B. Lidiard, Proc. Phys. Soc. London Sect. A **269**, 125 (1962).

31. F.F. Sizov and Yu.I. Ukhanov, *Magnetooptical Faraday and Voigt Effects in Application to Semiconductors* (Naukova Dumka, Kyiv, 1979) (in Russian).

32. Yu.I. Ukhanov, Sov. Phys. Usp. **16**, 236 (1973).

33. M. Poggio, R.C. Myers, N.P. Stern, A.C. Gossard, and D.D. Awschalom, Phys. Rev. B **72**, 235313 (2005).

34. W.J. Choyke and L. Patrik, Phys. Rev. **127**, 1868 (1962).

35. A.V. Komarov, S.M. Ryabchenko, and O.V. Terletskii, Phys. Status Solidi B **102**, 603 (1980).

36. W. Low and M. Weger, Phys. Rev. **118**, 1119 (1960).

Received 29.07.11.
Translated from Ukrainian by O.I. Voitenko

ЕФЕКТИ РОЗВЕДЕНОГО МАГНІТНОГО НАПІВПРОВІДНИКА В КАРБІДІ КРЕМНІЮ З ІМПЛАНТОВАНИМИ ІОНАМИ Mn I Fe

А.В. Комаров, А.В. Лось, С.М. Рябченко, С.М. Романенко

Р е з ю м е

Спектри пропускання і фарадеївського обертання площини поляризації світла, виміряні при температурі 2 K, порівняно для монокристалів 4H–SiC, імплантованих іонами Mn і 6H–SiC, імплантованих іонами Fe і контрольних зразків тих же монокристалів, що не піддавалися імплантації. Імплантацію проводили при енергії пучка 190 кеВ і з повними дозами опромінення $3,8{\cdot}10^{16}$ см$^{-2}$ і $5,5{\cdot}10^{16}$ см$^{-2}$. Вона приводить до створення поверхневих шарів з товщиною близько 0,2 мкм, легованих цими іонами, із середньою концентрацією іонів Mn або Fe близько 10^{21} см$^{-3}$. Пропускання світла через імплантовані кристали змінилося незначно у порівнянні з контрольними, що, однак, відповідало відносно великому коефіцієнту ослаблення світла в шарі з введеними іонами. Це інтерпретовано як результат розсіювання світла на неоднорідностях, створених потоком високоенергетичних іонів у цьому шарі. Присутність поверхневого шару, що містить магнітні іони, привело до значних змін у фарадеївському обертанні площини поляризації світла. Величини констант Верде для цього шару виявилися приблизно на три порядки більшими за модулем і протилежного знака в порівнянні з їх значеннями для контрольних зразків. Магнітопольові залежності фарадеївського обертання від шару з іонами Mn виявилися функціями поля, що насичуються. Це вказує на пропорційність фарадеївського обертання намагніченості парамагнітної підсистеми іонів Mn. У випадку шару, імплантованого іонами Fe, вони є лінійними за полем, подібно до того, як це спостерігається в $A^{II}FeB^{IV}$ напівмагнітних напівпровідниках. Зроблено припущення, що іони Fe у SiC, так як і у $A^{II}FeB^{IV}$, знаходяться у синглетному стані і набувають намагніченості у зовнішньому полі через механізм, подібний ван-флеківській намагніченості. Встановлено, що шари SiC із введеними іонами Mn або Fe демонструють магнітооптичні властивості, типові для розведених магнітних (напівмагнітних) напівпровідників. Разом з тим у вивчених (SiC,Mn)C і (SiC,Fe)C зразках не спостерігалося феромагнітного упорядкування.